MECHANICAL

TECHNOLOGY

INCORPORATED

GPO PRICE $ _____

CFSTI PRICE(S) $ _____

Hard copy (HC) 3.00

Microfiche (MF) .65

ff 653 July 65

FACILITY FORM 602

N67-17770
(ACCESSION NUMBER)

36
(PAGES)

CR 76226
(NASA CR OR TMX OR AD NUMBER)

1
(THRU)

15
(CATEGORY)

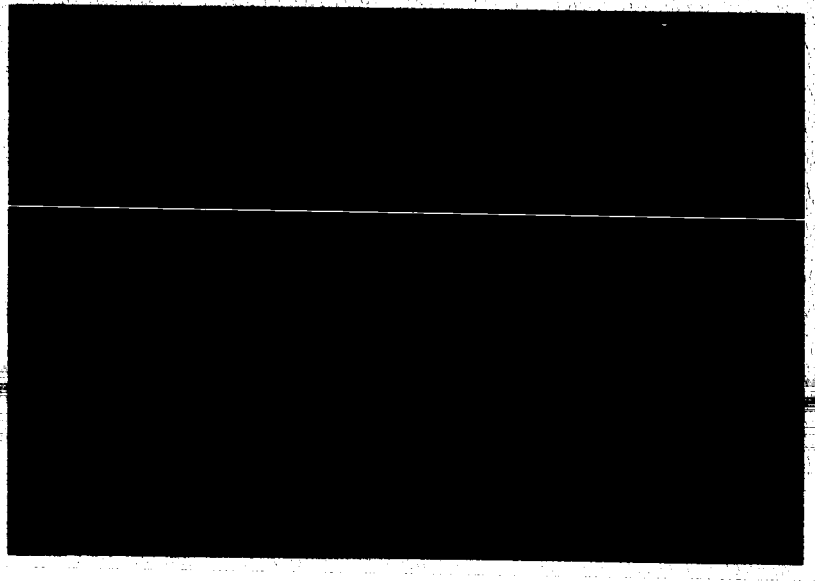

[redacted]and

AD738914

MECHANICAL TECHNOLOGY INCORPORATED
968 Albany-Shaker Road
Latham, New York 12110

MTI-66TR2

ON ERROR TORQUES OF SQUEEZE-FILM CYLINDRICAL JOURNAL BEARINGS

by

C.H.T. Pan
T. Chiang

January, 1966

NO. MTI-66TR2

DATE: January, 1966

TECHNICAL REPORT

ON ERROR TORQUES OF SQUEEZE-FILM CYLINDRICAL JOURNAL BEARINGS

by

C.H.T. Pan
T. Chiang

C. H. T. Pan T. Chiang

Author (s)

J. W. Lund

Approved

Ben Sternlicht

Approved

Prepared for

NATIONAL AERONAUTICS AND SPACE ADMINISTRATION
GEORGE C. MARSHALL SPACE FLIGHT CENTER
HUNTSVILLE, ALABAMA

Prepared under

Contract: NAS 8-11678

MTI
MECHANICAL TECHNOLOGY INCORPORATED

968 ALBANY - SHAKER ROAD — LATHAM, NEW YORK — PHONE 785-0922

TABLE OF CONTENTS

INTRODUCTION

In a single-axis gyroscope, the ideal gimbal axis suspension should be completely unrestrained. Considering the output axis, the read-out signal is usually the gyroscopic torque; if the suspension has a torque about the output axis, it would be included in the read-out measurement and would constitute an output error. Therefore in designing gimbal axis suspension system, it is of major importance to minimize its inherent torque, which will be called the error torque.

Fluid film bearings possessing perfect symmetry do not produce error torque, which, however, is often caused by manufacturing tolerances. In an externally pressurized gas bearing, for instance, causes for error torque include feeding flow unbalance, surface blemish, and gap ellipticity. It is reasonable to expect that error torque can be caused by manufacturing tolerances in a squeeze-film gas bearing in much the same way. This work is intended to gain some knowledge on the mechanisms and to develop means for estimating the magnitude of error torque in a squeeze-film bearing. A cylindrical geometry will be assumed for the bearing, and the squeeze frequency will be assumed to be sufficiently large to permit an asymptotic analysis (Ref. 2).

Three types of tolerance effects will be treated. Out-of-roundness of either the journal or the bearing or both would make the bearing gap non-uniform even when the bearing is unloaded. A third tolerance effect is related to the squeeze motion, in the event of dissymmetry in either the structure or the mounting constraints or the presence of appendages attached to the transducer of the squeeze-film bearing, the squeeze motion may lose rotational symmetry. An earlier study which treated only out-of-roundness in the bearing (Ref. 1) showed no resulting error torque. The present study will consider two additional effects as well as the interaction among the three.

BASIC EQUATIONS

Let us consider a cylindrical, squeeze-film journal bearing of finite length. Using cylindrical polar coordinates, the isothermal Reynolds' Equation is:

$$\frac{\partial}{\partial\theta}\left(H^3P\ \frac{\partial P}{\partial\theta}\right)+\frac{\partial}{\partial z}\left(H^3P\ \frac{\partial P}{\partial z}\right)=\sigma\ \frac{\partial}{\partial\tau}\ (PH) \qquad \ldots\ldots\ldots\ldots \quad (1)$$

where

$$\left.\begin{aligned}\sigma &= \frac{12\ \mu\ \Omega}{P_a}\left(\frac{R}{C}\right)^2 = \text{squeeze number}\\ \tau &= \Omega\ t = \text{dimensionless time}\\ z &= z^*/R = \text{dimensionless axial coordinate}\end{aligned}\right] \quad \ldots\ldots \quad (2)$$

Since the journal and the bearing are not perfectly circular in shape, we assume that the radii of the journal and the bearing can be expressed as $\left[R + e_1^* \cos 2(\theta-\alpha)\right]$ and $\left[R + C + e_2^* \cos 2(\theta-\beta)\right]$ respectively. Here, R is the mean radius of the journal, e_1^* and e_2^* represent the respective ellipticities, and α and β indicate the orientations of the respective major axes. Furthermore, we shall allow ellipticity in the squeeze motion. Thus, we can express the dimensionless film thickness

$$H = 1 + \varepsilon_o\left[1 + a\cos 2(\theta-\theta_1)\right]\cos\tau + \eta\cos\theta + \zeta\cos 2(\theta-\theta_2) \qquad \ldots\ldots\ldots\ldots \quad (3)$$

where

$$\zeta = \left[e_1^2 + e_2^2 - 2\,e_1 e_2\cos 2(\alpha-\beta)\right]^{\frac{1}{2}} \qquad \ldots\ldots\ldots\ldots$$

$$\theta_2 = \tfrac{1}{2}\tan^{-1}\frac{e_2\sin 2\beta - e_1\sin 2\alpha}{e_2\cos 2\beta - e_1\cos 2\alpha} \qquad \ldots\ldots\ldots\ldots \quad (4)$$

One can see from Eq. (4) that the last term of Eq. (3) is the combination of the journal and the bearing ellipticities. The quantity a is the ellipticity of excursion amplitude. When a = o, the squeeze motion is in its "hoop" mode of uniform excursion. The $\eta\cos\theta$ is the usual eccentricity term.

The boundary conditions of Eq. (1) are

$$P(z_1,\theta,\tau) = 1 \qquad \ldots\ldots\ldots\ldots \quad (5)$$

$$P(z_2,\theta,\tau) = 1 \qquad \ldots\ldots\ldots\ldots \quad (6)$$

$$P(z,\theta,\tau) = P(z,\theta+2\pi,\tau) \qquad \ldots\ldots\ldots\ldots \quad (7)$$

$$\frac{\partial P\ (z,\theta,\tau)}{\partial \theta} = \frac{\partial P\ (z,\theta + 2\pi,\tau)}{\partial \theta} \quad \ldots\ldots\ldots\ldots\ldots\ldots \quad (8)$$

In addition, P satisfies the condition of periodicity in time,

$$P\ (z,\theta,\tau) = P\ (z,\theta, + 2\pi) \quad \ldots\ldots\ldots\ldots\ldots\ldots \quad (9)$$

Since the squeeze number, σ, is typically very large, the asymptotic solution ($\sigma\to\infty$) is c interest. A general treatment of squeeze-film bearings using the asymptotic method is given in Reference 2. In Reference 3, a special application of this method is made for journal bearings. We shall recapitulate the asymptotic analysis in Appendix A for completeness. As $\sigma\to\infty$, Eq. (1) reduces to

$$\frac{\partial}{\partial \tau}(PH) = 0 \quad \ldots\ldots\ldots\ldots\ldots\ldots \quad (11)$$

or

$$\Psi = \Psi_\infty\ (z\ ,\theta), \quad \text{as } \sigma\to\infty \quad \ldots\ldots\ldots\ldots\ldots\ldots \quad (12)$$

where

$$\Psi \equiv PH \quad \ldots\ldots\ldots\ldots\ldots\ldots \quad (13)$$

The governing differential equation for Ψ_∞ is, as shown in Appendix A,

$$\frac{\partial}{\partial \theta}\left[\frac{\partial}{\partial \theta}(H_o \Psi_\infty^2) - 3\Psi_\infty^2 \frac{\partial H_o}{\partial \theta}\right] + \frac{\partial}{\partial z}\left[\frac{\partial}{\partial z}(H_o \Psi_\infty^2) - 3\Psi_\infty^2 \frac{\partial H_o}{\partial z}\right] = 0 \quad (14)$$

where H_o is the time-average of H,

$$H_o = \frac{1}{2\pi}\int_o^{2\pi} H\, d\tau$$

$$= 1 + \eta \cos\theta + \zeta \cos 2\ (\theta - \theta_2) \quad \ldots\ldots\ldots\ldots\ldots\ldots \quad (15)$$

The asymtptotic solution Ψ_∞ is a good approximation to the problem, except in the narrow regions near the edges. These narrow regions are referred to as the boundary layers; the extent of which is of the order of $1/\sqrt{\sigma}$.

The appropriate boundary conditions for Ψ_∞ at z_1 and z_2 are

$$\Psi_\infty^2\ (z_i,\ \theta) = \frac{\int_o^{2\pi} H^3\ (z_i,\theta,\tau)\, d\tau}{2\pi\ H_o(z_i,\theta)} \quad (i = 1,2) \quad \ldots\ldots\ldots\ldots \quad (16)$$

using a mass content rule derived in Appendix B.

Since both P and H and their first derivations are periodic in θ, we have

$$\Psi_\infty (z,\theta) = \Psi_\infty (z,\theta + 2\pi) \quad \ldots \quad (17)$$

$$\frac{\partial \Psi_\infty (z, \theta)}{\partial \theta} = \frac{\partial \Psi_\infty (z,\theta + 2\pi)}{\partial \theta} \quad \ldots \quad (18)$$

PERTURBATION SOLUTION - SMALL a, ζ, AND η.

The asymptotic solution Ψ_∞ governed by Eq. (14) and subject to boundary conditions (16), (17) and (18) will be solved in this section. For small a, ζ and η, we can solve the problem by the perturbation method and expand

$$\Psi_\infty^2 = G_o(z) + a\, G_1(z,\theta) + \zeta G_2(z,\theta) + \eta G_3(z,\theta) \quad . . . . . \quad (19)$$

Substituting Eq. (19) into Eq. (14) and collecting terms of the same power of a, ζ and η, we obtain

$$\frac{d^2G_o}{dz^2} = 0 \quad . . . . . \quad (20)$$

$$\frac{\partial^2 G_1}{\partial\theta^2} + \frac{\partial^2 G_1}{\partial z^2} = 0 \quad . . . . . \quad (21)$$

$$\frac{\partial^2 G_2}{\partial\theta^2} + \frac{\partial^2 G_2}{\partial z^2} = -8\, G_o \cos 2(\theta-\theta_2) \quad . . . . . \quad (22)$$

$$\frac{\partial^2 G_3}{\partial\theta^2} + \frac{\partial^2 G_3}{\partial z^2} = -2\, G_o \cos\theta \quad . . . . . \quad (23)$$

The boundary conditions are, from Eq. (16)

$$\Psi_\infty(z_i,\theta) = H_o^2(z_i,\theta) + \frac{3}{2}\,\varepsilon_o^2(z_i)\,[1 + a\cos 2(\theta-\theta_1)]^2$$

$$= [1 + \frac{3}{2}\,\varepsilon_o^2(z_i)] + a\,[3\,\varepsilon_o^2 \cos 2(\theta-\theta_1)]$$

$$+\zeta[2\cos 2(\theta-\theta_2)] + \eta[2\cos\theta] \quad . . . . . \quad (24)$$

Thus, we have the following boundary conditions (i = 1,2):

$$G_o(z_i) = 1 + \frac{3}{2}\,\varepsilon_o^2(z_i) \quad . . . . . \quad (25)$$

$$G_1(z_i,\theta) = 3\,\varepsilon_o^2 \cos 2(\theta-\theta_1) \quad . . . . . \quad (26)$$

$$G_2(z_i,\theta) = 2\cos 2(\theta-\theta_2) \quad . . . . . \quad (27)$$

$$G_3(z_i,\theta) = 2\cos\theta \quad . . . . . \quad (28)$$

In addition, we have the periodicity condition in θ for all G-functions. Now we assume that excursions are uniform in z, so that ε_o is a constant. The solutions subject to the above conditions are readily obtained.

$$G_o = 1 + \frac{3}{2}\,\varepsilon_o^2 \quad \ldots\ldots\ldots\ldots\ldots\ldots\ldots\ldots \quad (29)$$

$$G_1 = 3\,\varepsilon_o^2\,\frac{\cosh 2z}{\cosh 2\ell}\,\cos 2(\theta-\theta_1) \quad \ldots\ldots\ldots\ldots\ldots\ldots \quad (30)$$

$$G_2 = \left[2(1-G_o)\,\frac{\cosh 2z}{\cosh 2\ell} + 2G_o\right]\cos 2(\theta-\theta_2) \quad \ldots\ldots\ldots\ldots \quad (31)$$

$$G_3 = \left[2(1-G_o)\,\frac{\cosh z}{\cosh \ell} + 2G_o\right]\cos\theta \quad \ldots\ldots\ldots\ldots\ldots \quad (32)$$

where

$$z_1 = \frac{-L/2}{R} = -\ell\,; \quad z_2 = \frac{L/2}{R} = \ell \quad \ldots\ldots\ldots\ldots\ldots\ldots \quad (33)$$

Here, we have assumed that the bearing is of length L and the origin is taken at the middle plane (see Fig. 1).

The pressure distribution for the asymptotic problem (large σ) is obtained from:

$$P = \frac{\Psi_\infty}{H} = \frac{\sqrt{G_o}}{H_o + \varepsilon\cos\tau}\left\{1 + a\left[\frac{3}{2}\,\frac{\varepsilon^2{}_o}{G_o}\,\frac{\cosh 2z}{\cosh 2\ell}\,\cos 2(\theta-\theta_1)\right]\right.$$
$$+ \zeta\left[\frac{1-G_o}{G_o}\,\frac{\cosh 2z}{\cosh 2\ell} + 1\right]\cos 2(\theta-\theta_2)$$
$$\left. + \eta\left[\frac{1-G_o}{G_o}\,\frac{\cosh z}{\cosh \ell} + 1\right]\cos\theta\right\} \quad \ldots\ldots\ldots\ldots\ldots \quad (34)$$

where

$$\varepsilon = \varepsilon_o\,[1 + a\cos 2(\theta-\theta_1)] \quad \ldots\ldots\ldots\ldots\ldots\ldots \quad (35)$$

Torque Calculation

The torque acting on the journal is contributed jointly by the pressure force and by the viscous shear force.

A. Pressure Torque

It is clear that for a perfectly circular journal, the pressure force always passes through the center of the journal; consequently, there will be no torque due to the action of the pressure forces.

In order to calculate the pressure torque, let us first obtain an expression for the normal vector of an elliptic journal which is represented by

$$r = R + e_1^*\,\cos 2(\theta-\alpha) \quad \ldots\ldots\ldots\ldots\ldots\ldots \quad (36)$$

Denote the radial and circumferential unit vectors by $\vec{r}$ and $\vec{\theta}$, and tangential and normal unit vectors $\vec{t}$ and $\vec{n}$ (see Fig. 2). Thus,

$$\vec{t} = \vec{r}\frac{dr}{ds} + \vec{\theta}\frac{rd\theta}{ds} \quad \ldots \quad (37)$$

$$\vec{n} = \vec{r}\frac{rd\theta}{ds} - \vec{\theta}\frac{dr}{ds} \quad \ldots \quad (38)$$

where $ds = \sqrt{(dr)^2 + (rd\theta)^2}$

From Eq. (36) we have

$$dr = -2\, e_1^*\, \sin 2(\theta-\alpha)\, d\theta \quad \ldots \quad (39)$$

so that

$$ds = d\theta \sqrt{[2e_1^* \sin 2(\theta-\alpha)]^2 + r^2}$$

Substituting Eqs. (36) and (39) into (38),

$$\vec{n} = \vec{r}\frac{b_2}{\sqrt{b_1^2 + b_2^2}} + \vec{\theta}\frac{b_1}{\sqrt{b_1^2 + b_2^2}} \quad \ldots \quad (40)$$

where

$$\left.\begin{aligned} b_1 &= 2\, e_1^*\, \sin 2(\theta-\alpha) \\ b_2 &= R + e_1^*\, \cos 2(\theta-\alpha) \end{aligned}\right] \quad \ldots \quad (41)$$

Since the pressure force on element $rd\theta dz^*$ is acting in the negative $\vec{n}$-direction, its circumferential component may be expressed as

$$(-prd\theta dz^*\vec{n}) \cdot \vec{\theta} = -prd\theta dz^* \frac{b_1}{\sqrt{b_1^2 + b_2^2}} \quad \ldots \quad (42)$$

Now the time-averaged pressure torque is

$$T_p = \int_0^{2\pi} \frac{d\tau}{2\pi} \int_{L/2}^{L/2} dz^* \int_0^{2\pi} r\left[-prd\theta b_1 (b_1^2 + b_2^2)^{-\frac{1}{2}}\right] \quad . \quad (43)$$

Normalizing, we obtain

$$\frac{T_p}{p_a LDR} = -\frac{1}{4\pi L} \int_0^{2\pi} d\tau \int_{\ell}^{\ell} dz \int_0^{2\pi} \frac{r^2}{R} b_1 (b_1^2 + b_2^2)^{-\frac{1}{2}} P\, d\theta \quad \ldots \quad (44)$$

Integrate Eq. (44) with respect to τ, using Eq. (309) of Reference 4

$$\frac{T_p}{p_a LDR} = -\frac{1}{2L} \int_{\ell}^{\ell} dz \int_0^{2\pi} \frac{r^2}{R} b_1 (b_1^2 + b_2^2)^{-\frac{1}{2}} \frac{\Psi_\infty}{\sqrt{H_o - \varepsilon^2}}\, d\theta \quad \ldots \quad (45)$$

where $\varepsilon = \varepsilon_o [1 + a \cos 2 (\theta - \theta_1)]$ . . . . . (46)

Using Eq. (34) and integrating (45) with respect to z, we find

$$\frac{T_p}{p_a LDR} = -\frac{1}{2L} \sqrt{G_o} \int_o^{2\pi} \{2\ell + a \left[\frac{3}{2} \frac{\varepsilon^2_o}{G_o} \cos 2 (\theta - \theta_1) \tanh 2\ell \right] + \zeta \left[\frac{1-G_o}{G_o} \tanh 2\ell + 2\ell \right] \cos 2 (\theta - \theta_2) + \eta \left[2 \frac{1-G_o}{G_o} \tanh \ell + 2\ell \right] \cos\theta \}. \{ \frac{r^2}{R} \frac{b_1}{\sqrt{b_1^2 + b_2^2}} \cdot \frac{1}{\sqrt{H_o^2 - \varepsilon^2}} d\theta \quad . . . \quad (47)$$

Finally, neglecting $0 \{(\frac{C}{R})^2\}$, we integrate Eq. (47) and rearrange terms to obtain

$$\frac{T_p}{p_a LDR} = \frac{T_{p1}}{p_a LDR} + \frac{T_{p2}}{p_a LDR} \quad . . . . . \quad (48)$$

where

$$\frac{T_{p1}}{p_a LDR} = -(C/R)\, e_1\, a\, A_p \sin 2 (\theta_1 - \alpha)$$

$$\frac{T_{p2}}{p_a LDR} = (C/R) e_1\, \zeta\, A_p \sin 2 (\theta_2 - \alpha) \quad . . . . \quad (48a)$$

$$A_p = \pi \varepsilon_o^2 \sqrt{G_o}\, (1-\varepsilon_o^2)^{-\frac{1}{2}} \left[\frac{1}{1-\varepsilon_o^2} + \frac{3}{2} \frac{R}{L} \frac{1}{G_o} \tanh \frac{L}{R} \right]$$

Shear Torque

The time-averaged shear torque is

$$T_s = \int_o^{2\pi} \frac{d\tau}{2\pi} \int_{-L/2}^{L/2} dz^* \int_o^{2\pi} R\mu \frac{\partial u}{\partial y^*} \Big|_{y^* = 0} Rd\theta \quad . . . . . \quad (49)$$

where u is the velocity component in the θ-direction.

The θ-momentum equation is

$$\frac{\partial p}{R\partial\theta} = \mu \frac{\partial^2 u}{\partial y^{*2}} \quad \ldots\ldots\ldots\ldots\ldots\ldots\ldots\ldots \quad (50)$$

which is the same equation used to derive the Reynolds Equation (1). Note that in Eq. (50) we have neglected the non-linear convection terms for small Reynolds' number flow and the time-dependent term $\rho\frac{\partial u}{\partial t}$. Observe that the value of the ratio between $\rho \frac{\partial u}{\partial t}$ and $\mu \frac{\partial^2 u}{\partial y^{*2}}$ is of the order of $\frac{\Omega C^2}{\mu/\rho}$. For Ω= 20,000 cycles/sec, C = 10^{-4} in, $\frac{\mu}{\rho} = \frac{1}{6} \times 10^{-3}$ ft^2/sec, we obtain a typical value of $\frac{\Omega C^2}{\mu/\rho} = 0.06$. Therefore, the time-dependent terms in the momentum equation is indeed negligible even at this high-frequency oscillation.

Equation (50) together with the no-slip condition results in

$$u = \frac{C^2 p_a}{2\mu R} \frac{\partial P}{\partial\theta} \frac{y^*}{C} \left(\frac{y^*}{C} - H \right)$$

and

$$\left.\frac{\partial u}{\partial y^*}\right|_{y^* = 0} = - \frac{C p_a}{2R} \frac{\partial P}{\partial\theta} H \quad \ldots\ldots\ldots\ldots\ldots\ldots \quad (51)$$

Combining (49) and (51), and normalizing, we obtain

$$\frac{T_s}{p_a LDR} = - \frac{C}{8\pi LR} \int_0^{2\pi} d\tau \int_{L/2}^{L/2} dz^* \int_0^{2\pi} H \frac{\partial P}{\partial\theta} d\theta \quad \ldots\ldots\ldots \quad (52)$$

Note that in Eq. (49) we integrate the shear stress around the journal as if it were perfectly circular. It is seen from the above equation that the unit shear torque is of the order of $\frac{C}{R}$. A more accurate expression of the journal surface would only result in higher-order modification. Thus, Eq. (49) and consequently Eq. (52) are accurate to the first order of C/R.

Integrate Eq. (52) by parts,

$$\frac{T_s}{p_a LDR} = \frac{C}{8\pi LR} \int_0^{2\pi} d\tau \int_{-L/2}^{L/2} dz^* \int_0^{2\pi} P \frac{\partial H}{\partial\theta} d\theta$$

$$= \frac{C}{8\pi LR} \int_{-L/2}^{L/2} dz^* \int_0^{2\pi} d\theta \int_0^{2\pi} \frac{\Psi_\infty}{H_o + \varepsilon \cos\tau} \left(\frac{\partial H_o}{\partial\theta} + \frac{\partial \varepsilon}{\partial\theta} \cos\tau \right) d\tau \ldots \quad (53)$$

Now, integrate first with respect to τ then with respect to z* and θ. The result is

$$\frac{T_s}{p_a LDR} = \frac{C}{R}\, a\, \zeta\, A_s \sin 2(\theta_2 - \theta_1) \quad \ldots\ldots\ldots\ldots\ldots\ldots \quad (54)$$

$$A_s = \frac{\pi}{2}\sqrt{G_o}\left[(1-\varepsilon_o^2)^{-\frac{1}{2}} - 1 - \frac{R}{L}\,\frac{1-G_o}{G_o}\,\tanh\frac{L}{R}\right] \quad \ldots\ldots\ldots\ldots \quad (54a)$$

Thus, the total dimensionless torque is

$$\frac{T_{total}}{p_a LDR} = \frac{T_p}{p_a LDR} + \frac{T_s}{p_a LDR} \quad \ldots\ldots\ldots\ldots\ldots\ldots \quad (55)$$

with the right hand side given by Eqs. (48) and (54).

RESULTS

The combined ellipticity and phase angle (ζ and θ_2) of the journal and the bearing, as expressed by Eq. (4) are calculated and graphically shown in Figs. 3 and 4. The factors A_p and A_s of Eqs. (48) and (54) respectively, are plotted in Fig. 5 for various values of L/D. Both A_p and A_s increases with ε_o. A factor resembling A_p of Eq. (48) also appears in the unit radial stiffness calculation of Ref. 3. In fact, according to Ref. 3, the unit radial stiffness of a squeeze-film journal bearing is:

$$\frac{k_r C}{p_a LD} = 2\pi\varepsilon_o^2\sqrt{G_o}\,(1-\varepsilon_o^2)^{-\frac{1}{2}}\,\frac{1}{1-\varepsilon_o^2} + 3\,\frac{R}{L}\,\frac{1}{G_o}\tanh\frac{L}{2R} \quad \ldots\ldots (56)$$

where k_r is the radial stiffness. A comparison of Eqs. (48a) and (56) shows that the pressure torque is proportional to the unit stiffness of a bearing of twice the length. In Fig. 5, it is seen that the length effect is relatively small, thus one can conclude that the pressure torque is approximately proportional to the unit stiffness. Clearly, one way to obtain high stiffness is to have a large excursion ratio ε_o. In so doing, the pressure torque would be correspondingly "large". Fig. 5 shows that the shear torque also increases with ε_o. Thus for the same tolerances, any gain on the stiffness by increasing the excursion ratio is always accompanied by a penalty of increased error torque. The present analysis indicates that a bearing of high stiffness and low error torque can come about only through tolerance control in the absolute sense.

It is seen from Eqs. (48) and (54) that

1. If $e_1 = 0$ (no journal ellipticity), the "pressure torque" is zero. There would be a "shear torque" if both bearing and excursion ellipticities are present.
2. If $e_2 = 0$ (no bearing ellipticity), then $T_{p_2} = 0$. Both journal and excursion ellipticities are required for non-vanishing T_{p_1} and T_s.
3. If $a = 0$, (no excursion ellipticity), then $T_{p_1} = T_s = 0$. Combination of the journal and the bearing ellipticities may result in a pressure torque T_{p_2}.
4. Neither the "pressure torque" nor the "shear torque" are affected by the radial eccentricity.

The first part of pressure torque $\frac{T_{p1}}{p_a LRD}$ which is due to journal ellipticity and excursion ellipticity, is plotted in Fig. 6 as a function of θ_1 with the rest of the parameters fixed. It is obviously a double sine curve. Its value is zero when $\theta_1 = 0, 90^o, 180^o$, i.e. when the major (or minor) axis of excursion ellipticity coincides with either the major or the minor axis of journal ellipticity.

$\frac{T_{p2}}{p_a LDR}$ and $\frac{T_s}{p_a LDR}$ can, of course, be plotted similarly, but are omitted here.

The total dimensionless torque is plotted against β in Figure 7. Recall that θ_1 and β are the respective spatial phase angles indicating position relative to the journal ellipticity. It is therefore quite clear that once the transducer is mounted on the housing, there is a fixed spatial phase angle between $\theta 1$ and β. The various curves in Figure 7 are respectively for $\theta_1 = \beta, \beta + 45^o, \beta + 90^o, \beta + 135^o, \beta + 180^o$ with equal magnitudes in journal bearing and excursion ellipticities. The total dimensionless error torque is a minimum when $\theta_1 = \beta$ (or $\theta_1 = \beta + 180^o$), i.e. when the major axis of the excursion ellipticity coincides with the major axis of the bearing ellipticity, and a maximum when $\theta_1 = \beta + 90^o$.

For $e_1 = e_2 = a = e$ and $\alpha = 0$ we can show that

$$\zeta = e\{2(1 - \cos 2\beta)\}^{\frac{1}{2}} = 2e \sin\beta$$

$$\theta_2 = \tfrac{1}{2} \tan^{-1} \frac{2 \sin\beta \cos\beta}{\cos^2\beta - 1} = \tfrac{1}{2}\left(\frac{\pi}{2} + \beta\right)$$

$$\frac{T_{p1}}{p_a LDR} = \left(\frac{C}{R}\right) e^2 A_p \sin 2\theta_1$$

$$\frac{T_{p2}}{p_a LDR} = \left(\frac{C}{R}\right) e^2 A_p \sin 2\beta$$

$$\frac{T_s}{p_a LDR} = \left(\frac{C}{R}\right) 2 e^2 A_s \sin 2(\theta_2 - \theta_1) \sin\beta$$

$$= \left(\frac{C}{R}\right) e^2 A_s [\sin 2\theta_1 + \sin 2(\beta - \theta_1)]$$

Thus,

$$\frac{T_{total}}{p_a LDR} = \left(\frac{C}{R}\right) e^2 \{(A_s - A_p) \sin 2\theta_1 + A_p \sin 2\beta + A_s \sin 2(\beta - \theta_1)\} \quad \ldots\ldots\ldots\ldots\ldots \quad (57)$$

For a given spatial phase angle between β and θ_1, the last term of (57) is a constant. In Figure 7, the curves for $\theta_1 = \beta + 45^o$ and $\theta_1 = \beta + 135^o$ have a non-zero mean value which is represented by the last term of Eq. (57). Physically, this means that there is a torque in the average sense acting on the journal. The journal will rotate in the direction according to the sign of the mean torque.

Consider the situation that the transducer is mounted on the bearing housing with perfect symmetry. The excursion ellipticity of the transducer is caused exclusively by the non-uniformity in transducer wall thickness (see Figure 8). It is seen from Appendix C that the "hoop" mode of vibration of the transducer is slightly distorted. The excursion amplitude of the thinner regions (A and B) of Figure 8 is slightly greater than that of the thicker regions (C and D of Figure 8). Thus, θ_1 is equal to β and the magnitude of the error torque would be the minimum possible according to Fig. 7. Even so, the magnitude of the error torque for the AB-5 bearing with R = 2.75 cm, operating in an atmospheric ambient would be about 40 dyne-cm. This estimate should be about one order of magnitude too conservative since actual tolerances would have axial variation and the net effect should be much smaller in magnitude than that due to an axially uniform tolerance.

CONCLUSIONS

On the basis of the analysis and the results considered in the previous sections, we conclude the following:

1. The asymptotic analysis of squeeze-film bearings is suitable for studying error torque when σ is sufficiently large. The inaccuracy involved in the asymptotic analysis is of the order of $1/\sqrt{\sigma}$.

2. A first estimate of the error torque can be obtained by an asymptotic analysis considering perturbation effects of gap and excursion ellipticities.

3. Both pressure and shear stress at the journal surface can cause error torque. Within the accuracy of the asymptotic perturbation analysis, the "pressure torque" requires both gap and excursion ellipticities. Also, radial eccentricity does not affect error torque directly.

4. The magnitude of the error torque is proportional to C/R and increases with ε_o. The "pressure torque" is directly proportional to stiffness of a bearing of double length.

5. The total magnitude of the error torque depends on the individual magnitude of each of the three types of ellipticities and the relative orientations of their major axes. In particular, if the magnitudes of the three types of ellipticities are equal, the magnitude of the total torque is largest when the major axis of the bearing ellipticity coincides with the minor axis of the excursion ellipticity, and is smallest when the respective major axes coincide. In either case the total torque is doubly periodic with the angle between the major axes of the journal and bearing ellipticities with zero average. If the principal axes of the bearing and excursion ellipticities do not coincide, then the torque would have a non-zero average so that the journal would rotate continuously.

6. Reduction of error torque without corresponding reduction in stiffness can be most effectively realized by absolute tolerance control.

APPENDIX A: ASYMPTOTIC APPROXIMATION

Rewrite Eq. (1) in the form

$$\frac{\partial}{\partial \tau}\ (PH) = \frac{1}{\sigma}\ \left\{\frac{\partial}{\partial \theta}\ (H^3P\ \frac{\partial P}{\partial \theta}\ ) + \frac{\partial}{\partial z}\ (H^3P\ \frac{\partial P}{\partial z}\ )\right\} \quad \ldots\ldots\ldots\ldots\ldots\ldots \quad (A\text{-}1)$$

$$\text{As } \sigma \to \infty,\ \frac{\partial}{\partial \tau}\ (PH) = 0 \quad \ldots\ldots\ldots\ldots\ldots\ldots\ldots\ldots\ldots\ldots\ldots \quad (A\text{-}2)$$

$$\text{or } \Psi = \Psi_\infty\ (z,\theta) \quad \ldots\ldots\ldots\ldots\ldots\ldots\ldots\ldots\ldots\ldots\ldots \quad (A\text{-}3)$$

$$\text{where } \Psi \equiv PH \quad \ldots\ldots\ldots\ldots\ldots\ldots\ldots\ldots\ldots\ldots\ldots \quad (A\text{-}4)$$

When $\sigma \to \infty$, the right hand side of Eq. (A-1) which contains all the space deviations, vanishes; this clearly indicates a singular perturbation phenomenon. The asymptotic solution Ψ_∞ is not uniformly valid throughout the whole bearing film. More specifically, in the narrow regions near the edges, $z = z_1$ and $z = z_2$, the gradient (z-deviatives) may be so steep that in Eq. (A-1) the term $\frac{1}{\sigma}\frac{\partial}{\partial z}\ (H^3P\ \frac{\partial P}{\partial z}\ )$ is of the same order as $\frac{\partial}{\partial \tau}\ (\Psi)$.

These narrow regions are called the boundary layers; the extent of which is of the order of $\frac{1}{\sqrt{\sigma}}$. Let Ψ_e be the edge correction in the boundary layers, then

$$\Psi = \Psi_e\ (z,\theta,\tau) + \Psi_\infty\ (z,\theta) \quad \ldots\ldots\ldots\ldots\ldots\ldots\ldots\ldots \quad (A\text{-}5)$$

In the interior of the film (outside the boundary layers), $\Psi=\Psi_\infty$ is a good approximation, since Ψ_e is important only in the boundary layers.

During the process of reduction from Eq. (A-1) to Eq. (A-2), the differential equation loses two orders in z-differentiation, consequently, the asymptotic solution Ψ_∞ will not satisfy the two boundary conditions (5) and (6), page 2 . The boundary conditions to be satisfied by Ψ_∞ at z_1 and z_2 can only be determined by a mass content rule which will be discussed later.

Integrating Eq. (A-1) with respect to τ from o to 2π we obtain

$$\int_o^{2\pi} \frac{\partial}{\partial \theta}\left[\frac{\partial}{\partial \theta}\ (H\Psi^2) - 3\Psi^2\ \frac{\partial H}{\partial \theta}\right] d\tau + \int_o^{2\pi} \frac{\partial}{\partial z}\left[\frac{\partial}{\partial z}\ (H\Psi^2) - 3\Psi^2\ \frac{\partial H}{\partial z}\right] d\tau = 0 \quad (A\text{-}6)$$

The following identity has been used

$$H^3P\ d\ P = \tfrac{1}{2}\ d\ (H\Psi^2) - \frac{3}{2}\ \Psi^2 dH \quad \ldots\ldots\ldots\ldots\ldots\ldots \quad (A\text{-}7)$$

Neglecting the edge correction Ψ_e and using the asymptotic approximation, Eq. (A-6) is readily reduced to

$$\frac{\partial}{\partial\theta}\left[\frac{\partial}{\partial\theta}(H_o\Psi_\infty^2) - 3\Psi_\infty^2\frac{\partial H_o}{\partial\theta}\right] + \frac{\partial}{\partial z}\left[\frac{\partial}{\partial z}(H_o\Psi_\infty^2) - 3\Psi_\infty^2\frac{\partial H_o}{\partial z}\right] = 0 \quad . \quad . \quad . \quad (A\text{-}8)$$

where H_o is the time-average of H,

$$H_o = \frac{1}{2\pi}\int_o^{2\pi} H\, d\,\tau$$

$$= 1 + \eta\cos\theta + \zeta\cos 2\,(\theta-\theta_2) \quad . \quad . \quad . \quad . \quad . \quad . \quad . \quad . \quad . \quad . \quad . \quad . \quad . \quad . \quad . \quad . \quad . \quad (A\text{-}9)$$

The θ-wise boundary conditions require that both Ψ_∞ and its derivative with respect to θ be periodic in θ. The z-wise boundaries, however, are not known explicitely. Equation (5) and (6) are not useful because at $z = z_1$ and $z = z_2$ the edge correction Ψ_e is important but unknown. In the following section a mass content rule will be derived which may be used as boundary conditions for Ψ_∞ at z_1 and z_2.

APPENDIX B: BOUNDARY CONDITIONS FOR Ψ_∞.

The boundary conditions for the asymptotic solution are derived in this section. We first integrate Eq. (A-6) with respect to z,

$$\int_0^{2\pi} \left[\frac{\partial}{\partial z}(H\Psi^2) - 3\Psi^2 \frac{\partial H}{\partial z}\right] d\tau + \int_{z_1}^{z} dz' \int_0^{2\pi} d\tau \frac{\partial}{\partial \theta}\left[\frac{\partial}{\partial \theta}(H\Psi^2) - 3\Psi^2 \frac{\partial H}{\partial \theta}\right] = A(\theta). \quad \text{(B-1)}$$

where $A(\theta)$ is an integration "constant".

Integrate (B-1) with respect to z again,

$$\int_0^{2\pi} H\Psi^2 d\tau = A(\theta)\, z + B(\theta) + I(z,\theta) \quad \text{(B-2)}$$

where

$$I(z,\theta) = 3\int_{z_1}^{z} dz' \int_0^{2\pi} d\tau\, \Psi^2 \frac{\partial H}{\partial z'}$$

$$- \int_{z_1}^{z} dz' \int_{z_1}^{z'} dz'' \int_0^{2\pi} d\tau \frac{\partial}{\partial \theta}\left[\frac{\partial}{\partial \theta}(H\Psi^2) - 3\Psi^2 \frac{\partial H}{\partial \theta}\right] \quad \text{(B-3)}$$

and $B(\theta)$ is another integration "constant".

On the boundary we have, from Eqs. (5) and (6),

$$\Psi(z_i,\theta,\tau) = H(z_i,\theta,\tau) \qquad (i=1,2) \quad \text{(B-4)}$$

Evaluate Eq. (B-2) on the boundary,

$$\int_0^{2\pi} H^3(z_i,\theta,\tau)\, d\tau = A(\theta)\, z_i + B(\theta) + I(z_i,\theta) \quad \text{(B-5)}$$

Now we use the asymptotic approximation and replace Ψ by Ψ_∞ on the left hand side of Eq. (B-2).

$$\Psi_\infty^2(z,\theta) \int_0^{2\pi} H d\tau = A(\theta)\, z + B(\theta) + I(z,\theta) \quad \text{(B-6)}$$

Let δz_1 be the boundary layer thickness at z_1, then we can evaluate Eq. (B-6) at $z = z_1 + \delta z_1$,

$$\Psi_\infty^2(z_1 + \delta z_1, \theta)\, 2\pi H_o(z_1 + \delta z_1, \theta) = A(\theta)(z_1 + \delta z_1) + B(\theta) + I(z_1 + \delta z_1, \theta) \quad \text{(B-7)}$$

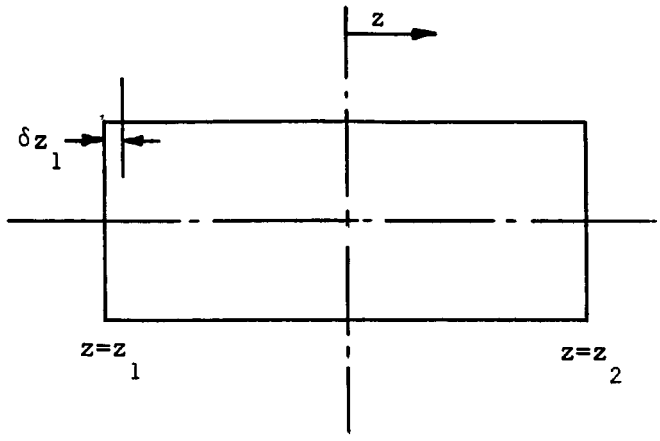

Figure B-1

Since δz_1 is of the order of $(\sigma^{-\frac{1}{2}})$, the right hand sides of Eq. (B-7) with i = 1 are equal if terms of 0 $(\sigma^{-\frac{1}{2}})$ are neglected. Thus, a comparison of (B-5) and (B-7) leads to

$$\int_0^{2\pi} H^3 (z_2, \theta,\tau)\, d\tau = \Psi_\infty^2 (z_1 + \delta z_1,\theta) \int_0^{2\pi} H (z_1 + \delta z_1,\theta,\tau)\, d\tau \quad \ldots (B\text{-}8)$$

Since δz_1 is small, it is reasonable that we impose the value of Ψ_∞ at z_1 to be that at $z_1 + \delta z_1$.

Thus,

$$\Psi_\infty (z_1 + \delta z_1,\theta) = \Psi_\infty(z_1,\theta) \quad \ldots\ldots\ldots\ldots\ldots\ldots\ldots (B\text{-}9)$$

Substituting (B-9) into Eq. (B-8), we obtain

$$\Psi_\infty^2 (z_1,\theta) = \frac{\int_0^{2\pi} H^3(z_1,\theta,\tau)\, d\tau}{2\pi H_o (z_1,\theta)} \quad \ldots\ldots\ldots\ldots\ldots\ldots\ldots (B\text{-}10)$$

Similarly,

$$\Psi_\infty^2 (z_2,\theta) = \frac{\int_0^{2\pi} H^3 (z_2,\theta,\tau)\, d\tau}{2\pi H_o (z_2,\theta)} \quad \ldots\ldots\ldots\ldots\ldots\ldots\ldots (B\text{-}11)$$

APPENDIX C: EXCURSION MODES OF A TRANSDUCER

The excursion modes of the transducer shown in Fig. 8 will be analyzed here according to a simplified model.

While the analysis is only approximate, its purpose is to find out whether the thicker regions or the thinner regions have larger excursion amplitude at its distorted "hoop" mode.

Using the lumped-parameter method, the masses of the thicker and the thinner ends are represented by $(m + \delta m)$ and $(m - \delta m)$ respectively (see Figure C-1). From the geometrical configuration of Fig. 8 it is evident that the masses $(m + \delta m)$ are supported by weaker spring $(k - \delta k)$ and the smaller masses $(m - \delta m)$ are supported by stronger springs $(k + \delta k)$. The four springs with springs with spring constant, say, k connecting the masses serve the purpose of providing the coupling between the respective masses.

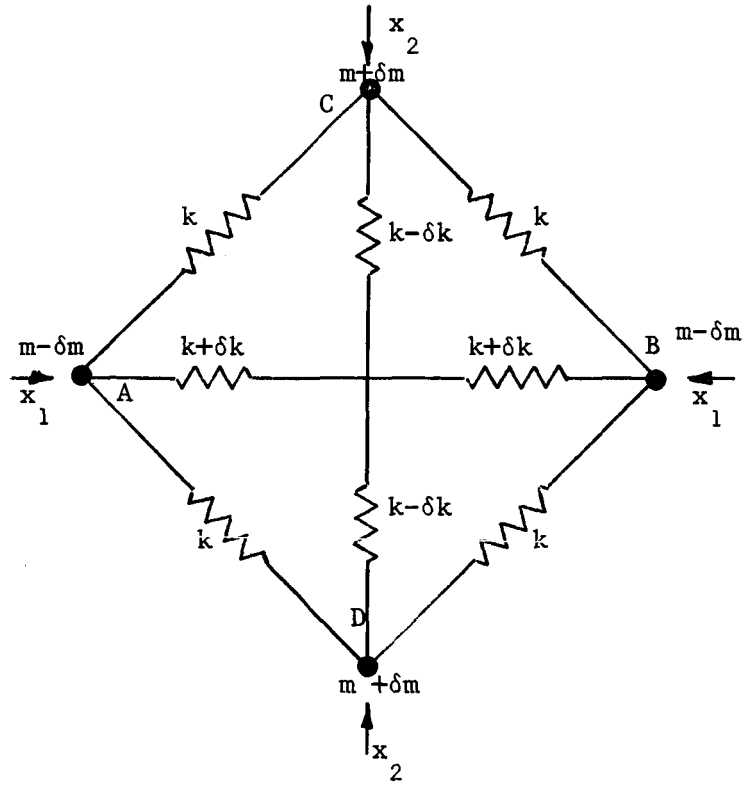

Fig. C-1 Lumped-parameter diagram for the transducer shown in Fig. 8.

In analyzing the small vibrations of the system, let us assume that

$$x_1 = \text{displacement of } m - \delta m$$
$$x_2 = \text{displacement of } m + \delta m \qquad \ldots\ldots\ldots\ldots\ldots\ldots \quad (C\text{-}1)$$

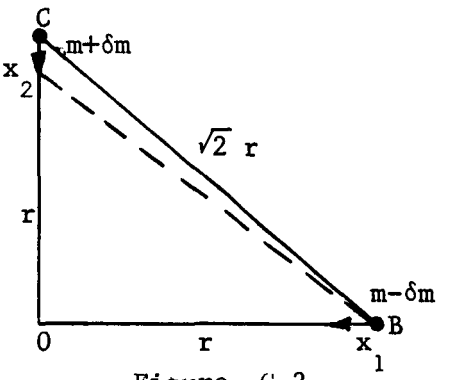

Figure C-2

Now consider the geometry of masses C and B with center position of the system "0" as shown in Figure C-2. The lengths of the respective element are also shown there. Now let the mass A have a displacement x_2. Then the reduction of length of the spring CB is

$$\sqrt{2}\, r - \sqrt{r^2 + (r - x_2)^2} = \sqrt{2}\, r - \sqrt{2}\, r \left(1 - \frac{1}{2}\,\frac{x_2}{r}\right) = \frac{\sqrt{2}}{2}\, x_2$$

neglecting the higher-order terms of $\frac{x_2}{r}$.

Similarly, due to a displacement x_1 at B, the spring CB reduces its length by an amount of $\frac{\sqrt{2}}{2}\, x_1$. Now we are ready to write the equation of motion for $(m - \delta m)$,

$$(m - \delta m)\, \ddot{x}_1 + (k + \delta k)\, x_1 + 2 \left\{k\, \frac{\sqrt{2}}{2}\, (x_1 + x_2)\, \frac{\sqrt{2}}{2} = 0\right.$$

The last factor $\frac{\sqrt{2}}{2}$ stands for taking the component of the spring forces along the x_1 - direction. Rearranging we have $(m - \delta m)\, \ddot{x}_1 + (k + \delta k)\, x_1 + k(x_1 + x_2) = 0$. (C-2)

Similarly, the equation of motion of $(m + \delta m)$ is

$$(m + \delta m)\, \ddot{x}_2 + (k - \delta k)\, x_2 + k\, (x_1 + x_2) = 0 \qquad \ldots\ldots\ldots\ldots \quad (C\text{-}3)$$

Assume that x_1 and x_2 are of the form

$$\left.\begin{aligned} x_1 &= c_1 \sin(\omega t + \bar{\alpha}) \\ x_2 &= c_2 \sin(\omega t + \bar{\alpha}) \end{aligned}\right] \qquad \ldots\ldots\ldots\ldots\ldots\ldots\ldots\ldots \quad (C\text{-}4)$$

where c_1 and c_2 are the amplitudes and ω, the frequency.

Substitution of (C-4) into Eq. (C-2) and (C-3) yields

$$\left(-\omega^2 + \frac{2k + \delta k}{m - \delta m}\right) C_1 + \frac{k}{m - \delta m} C_2 = 0 \quad \text{. . . . . (C-5)}$$

$$\frac{k}{m + \delta m} C_1 + \left(-\omega^2 + \frac{2k - \delta k}{m + \delta m}\right) C_2 = 0 \quad \text{. . . . . (C-6)}$$

Since (C-5) and (C-6) is a set of two homogeneous equations, the determinant of the coefficients must vanish. Expansion of the determinant results in

$$\omega^2 = \frac{2k}{m}\left(1 + \frac{1}{2}\frac{\delta m\, \delta k}{mk} + \frac{(\delta m)^2}{m^2}\right) \pm \frac{k}{m}\left(1 + 2\frac{\delta m\, \delta k}{mk} + \frac{5}{2}\frac{(\delta m)^2}{m^2} + \frac{1}{2}\frac{(\delta k)^2}{k^2}\right) \quad \text{. . . . . (C-7)}$$

neglecting the higher-order terms of $\frac{\delta m}{m}$ and $\frac{\delta k}{k}$. It is seen from (C-7) that the characteristic frequency ω of the system is modified only in the second-order in $\frac{\delta m}{m}$ and $\frac{\delta k}{k}$.

Therefore we have, to the first order,

$$\omega^2 = \frac{2k}{m} \pm \frac{k}{m} \quad \text{. . . . . (C-8)}$$

Take the plus sign in (C-8) which, as we shall see later, corresponds to the distorted "hoop" mode,

$$\omega = \sqrt{\frac{3k}{m}} \quad \text{. . . . . (C-9)}$$

Substituting (C-9) into (C-5) and keeping terms up to the first order, we obtain

$$\frac{C_1}{C_2} = 1 + \frac{\delta k}{k} + 3\frac{\delta m}{m} \quad \text{. . . . . (C-10)}$$

Since δk and δm are positive quantities,

$$\frac{C_1}{C_2} > 1 > 0 \quad \text{. . . . . (C-11)}$$

Equations (C-10) and (C-11) clearly indicate a distorted "hoop" mode of vibration, the mass $(m - \delta m)$ has larger amplitude than the mass $(m + \delta m)$. Going back to Fig. 8, the thinner regions of the transducer have larger amplitude than the thicker regions at its distorted "hoop" mode of vibration.

NOMENCLATURE

a	ellipticity in excursion
A, B	integration constants
A_p, A_s	defined in Equations (48a) and (54a)
b_1, b_2	defined in Equation (41)
C	radial clearance
D	bearing diameter
e_1^*, e_2^*	ellipticities of the journal and the bearing
e_1, e_2	dimensionless ellipticities, $\frac{e_1^*}{C}$, $\frac{e_2^*}{C}$
F	bearing force
G_o, G_1, G_2, G_3	defined in Equation (19)
H^*	bearing film thickness
H	dimensionless film thickness, H^*/C
H_o	defined in Equation (15)
I	defined in Equation (B-3)
L	bearing length
ℓ	$L/2R$
p	pressure
p_a	ambient pressure
P	dimensionless pressure p/p_a
R	mean randius of journal
T	torque
T_p	pressure torque
T_{p1}, T_{p2}	defined in Equation (48a)
T_s	shear torque
T_{total}	total torque
t	time

u	velocity in θ-direction
y^*	coordinate perpendicular to journal surface
z^*	axial coordinate
z	dimensionless axial coordinate, z^*/R
z_1	$-\frac{L/2}{R}$
z_2	$\frac{L/2}{R}$
α, β	spatial phase angles indicating relative orientation of journal and bearing
ε_o^*	amplitude of excursion
ε_o	normalized excursion amplitude, ε_o^*/C
ε	$\varepsilon_o [1 + a \cos 2 (\theta-\theta_1)]$
ζ	combined ellipticity, defined in Eq. (4)
η	eccentricity (normalized with respect to C)
θ	angular coordinate
θ_1	spatial phase angle of excursion ellipticity
θ_2	spatial phase angle of combined ellipticity of journal and bearing, defined in Eq.(4).
μ	viscosity
ρ	density
σ	squeeze number = $\frac{12\mu\Omega}{p_a} \left(\frac{R}{C}\right)^2$
τ	dimensionless time, Ωt
Ψ	PH
Ψ_∞	asymptotic solution of Ψ
Ω	squeeze frequency

REFERENCES

1. Pan, C.H.T., Editor, "Analysis, Design and Prototype Development of Squeeze-Film Bearings for AB-5 Gyro", MTI Report 64-TR-66, Section IV-B, November, 1964.
2. Pan, C.H.T. "On Asymptotic Analysis of Gaseous Squeeze-Film Bearings", MTI-65TR20, April, 1965.
3. Pan, C.H.T. and Malanoski, S., "The Solution of Special Squeeze-Film Gas Bearing Problems by an Improved Numerical Technique", MTI-65TR26, to be issued.
4. Peirce, B.O., "A Short Table of Integrals", Ginn and Company, 1956.

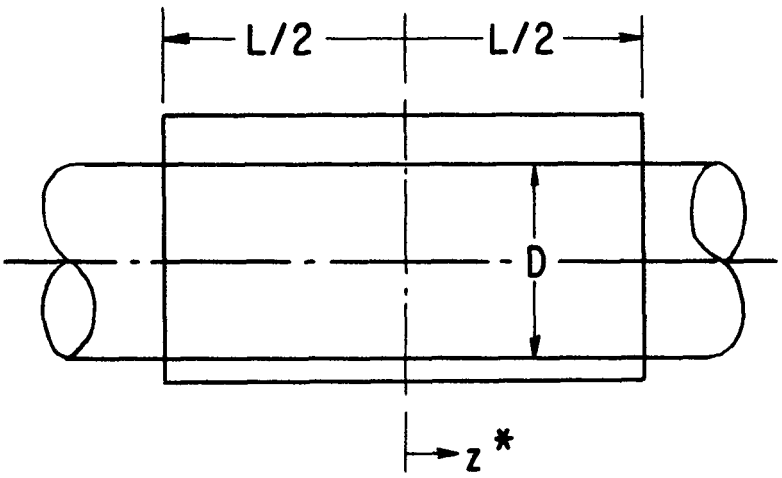

Fig. 1 Cylindrical Journal Squeeze-Film Bearing Configuration

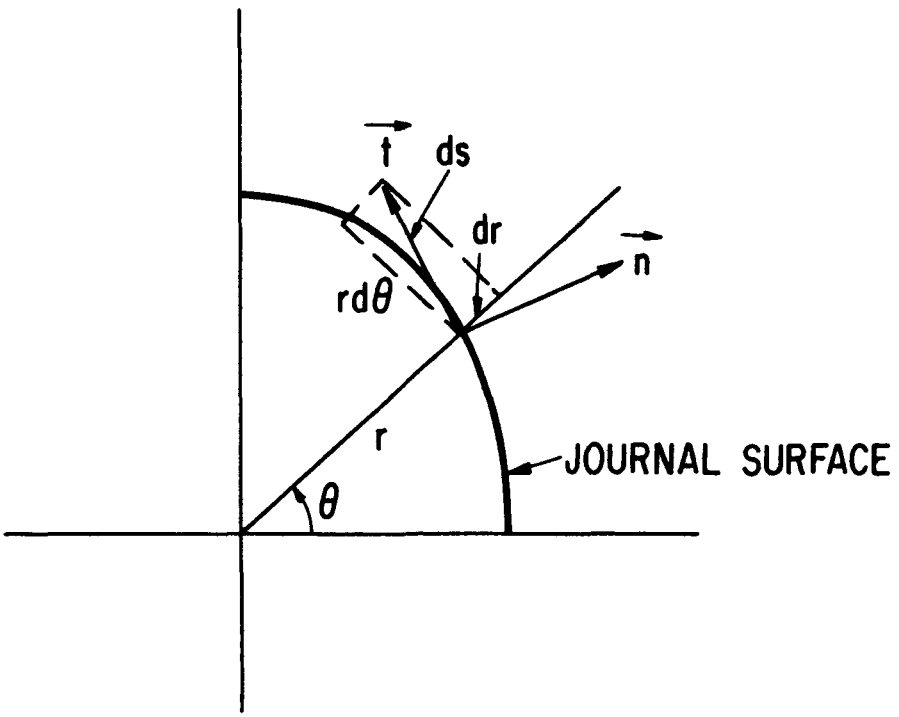

Fig. 2 Elliptical Journal Geometry

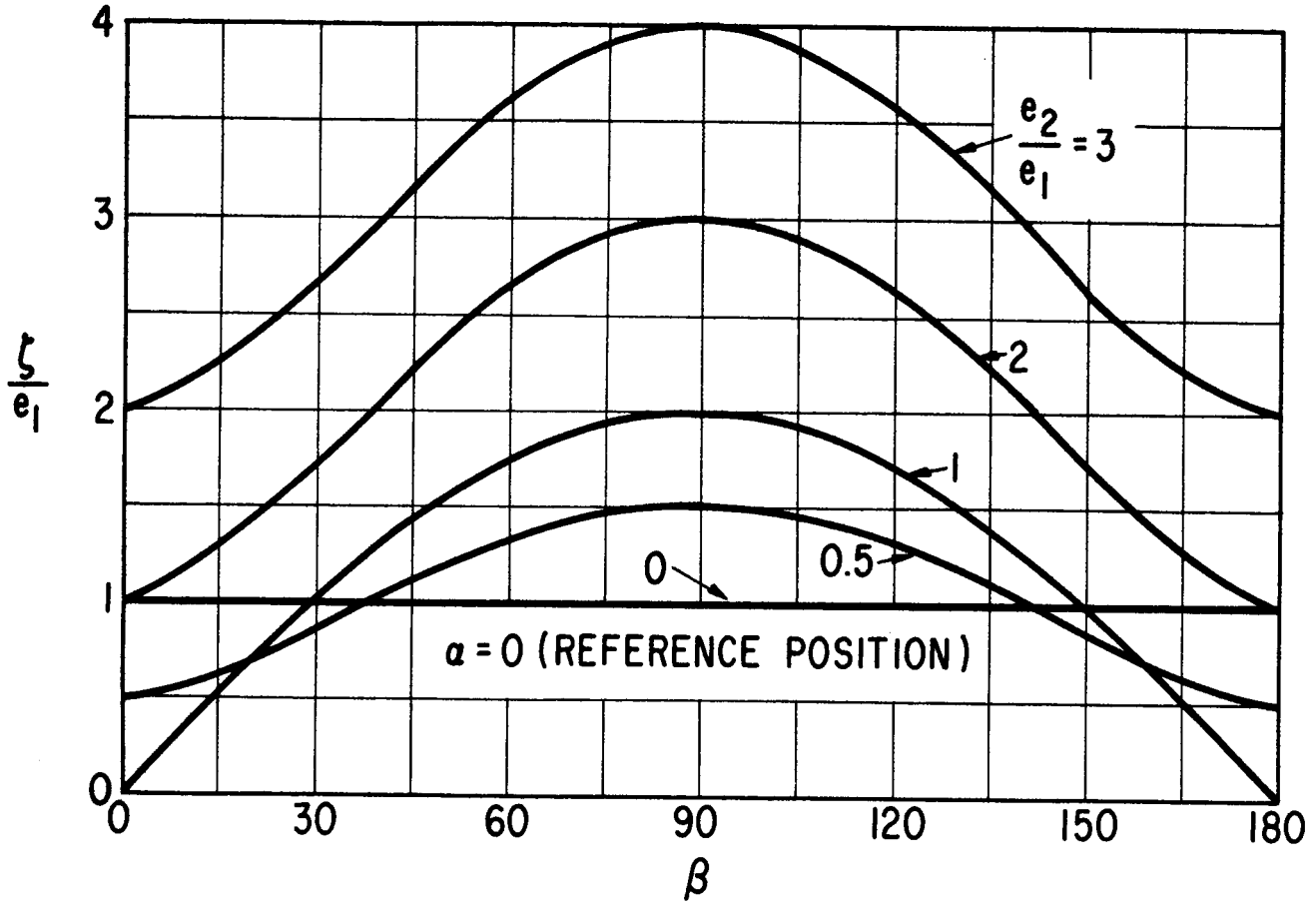

Fig. 3 $\frac{\zeta}{e}$ against β for various $\frac{e_2}{e}$

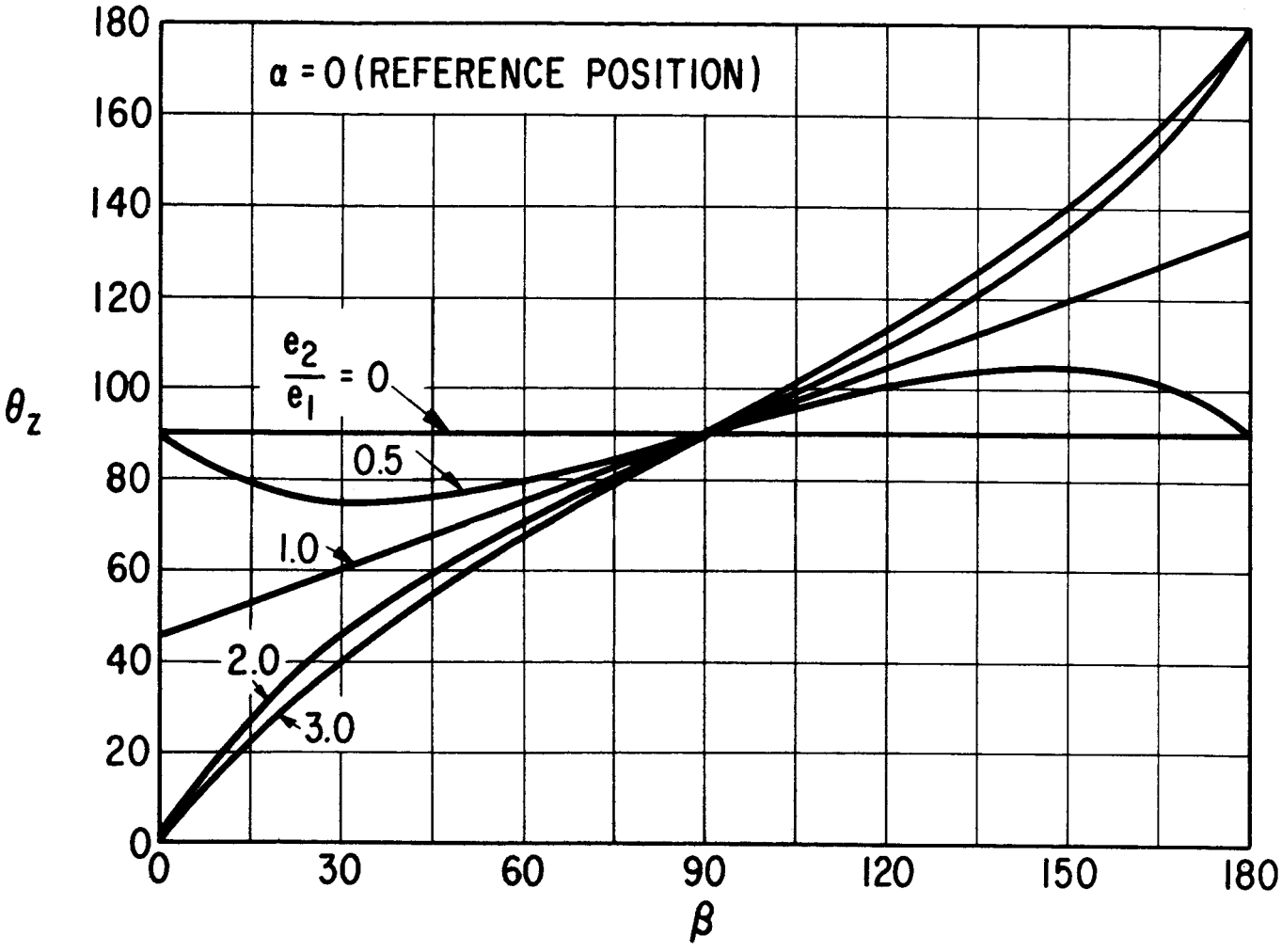

Fig. 4 θ_2 against β for various $\frac{e_2}{e_1}$

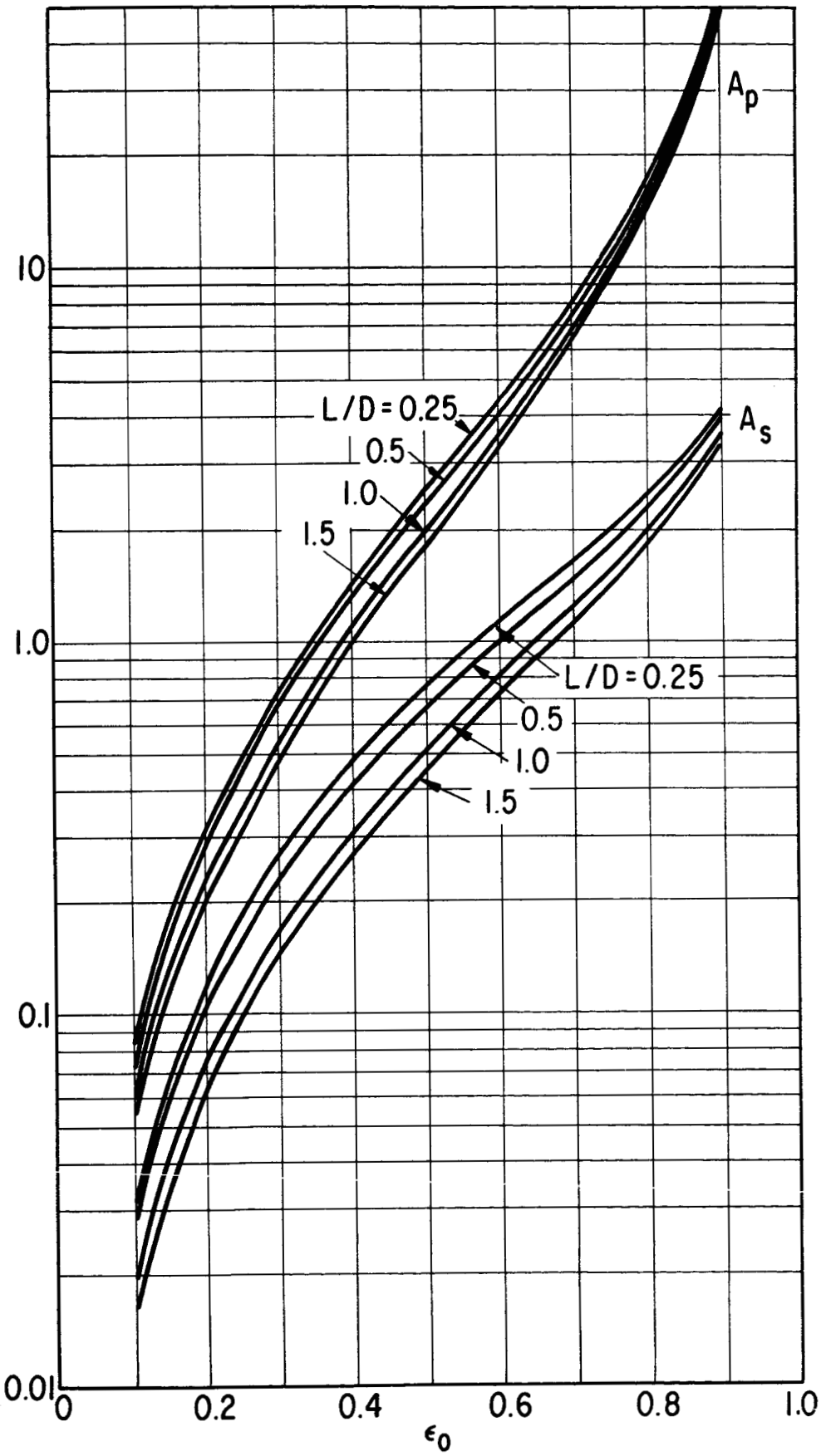

Fig. 5 A_p and A_s versus ε_o for various L/D

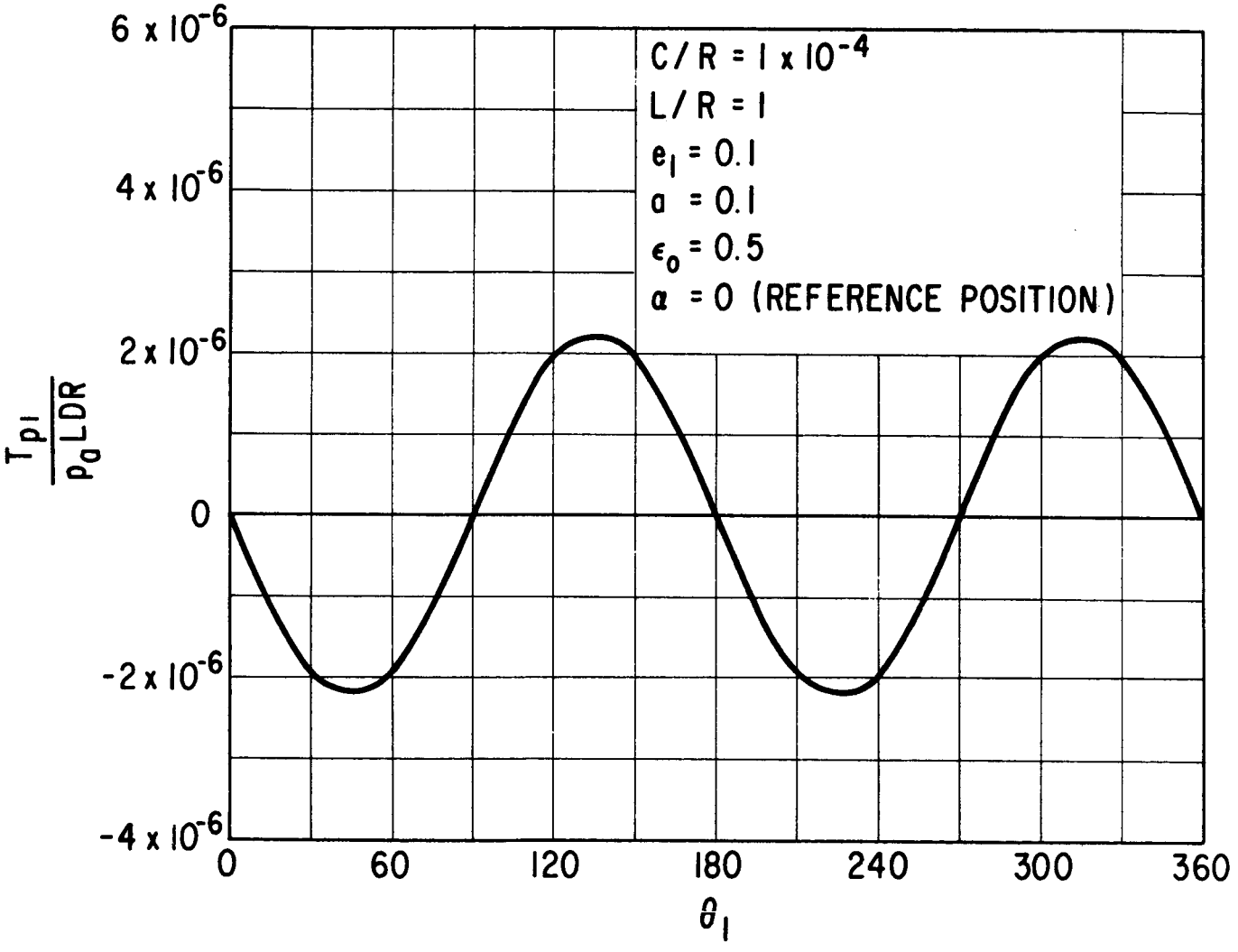

Fig. 6 $\frac{T_{p1}}{p_a LDR}$ versus θ_1

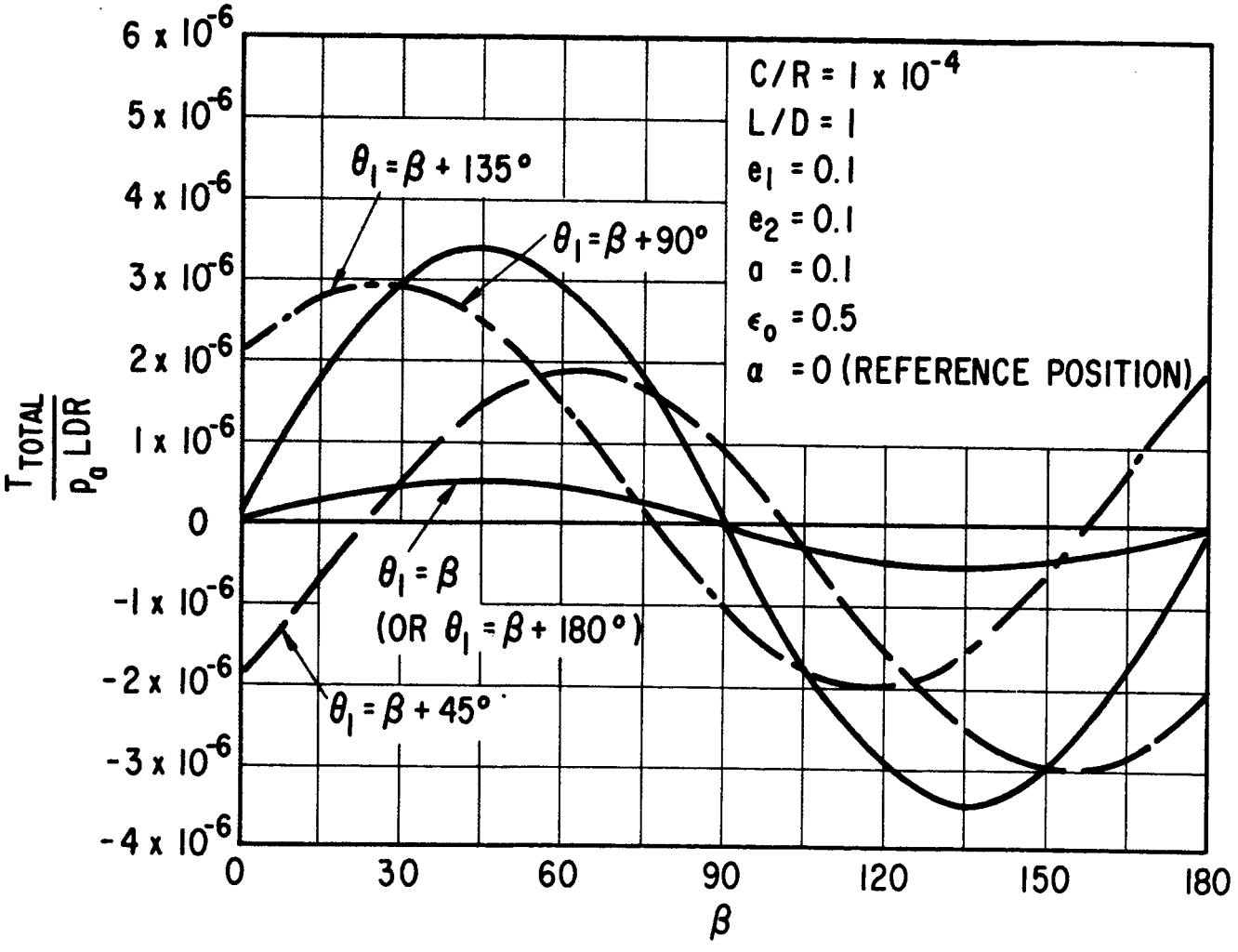

Fig. 7 $\frac{T_{total}}{p_a LDR}$ versus β

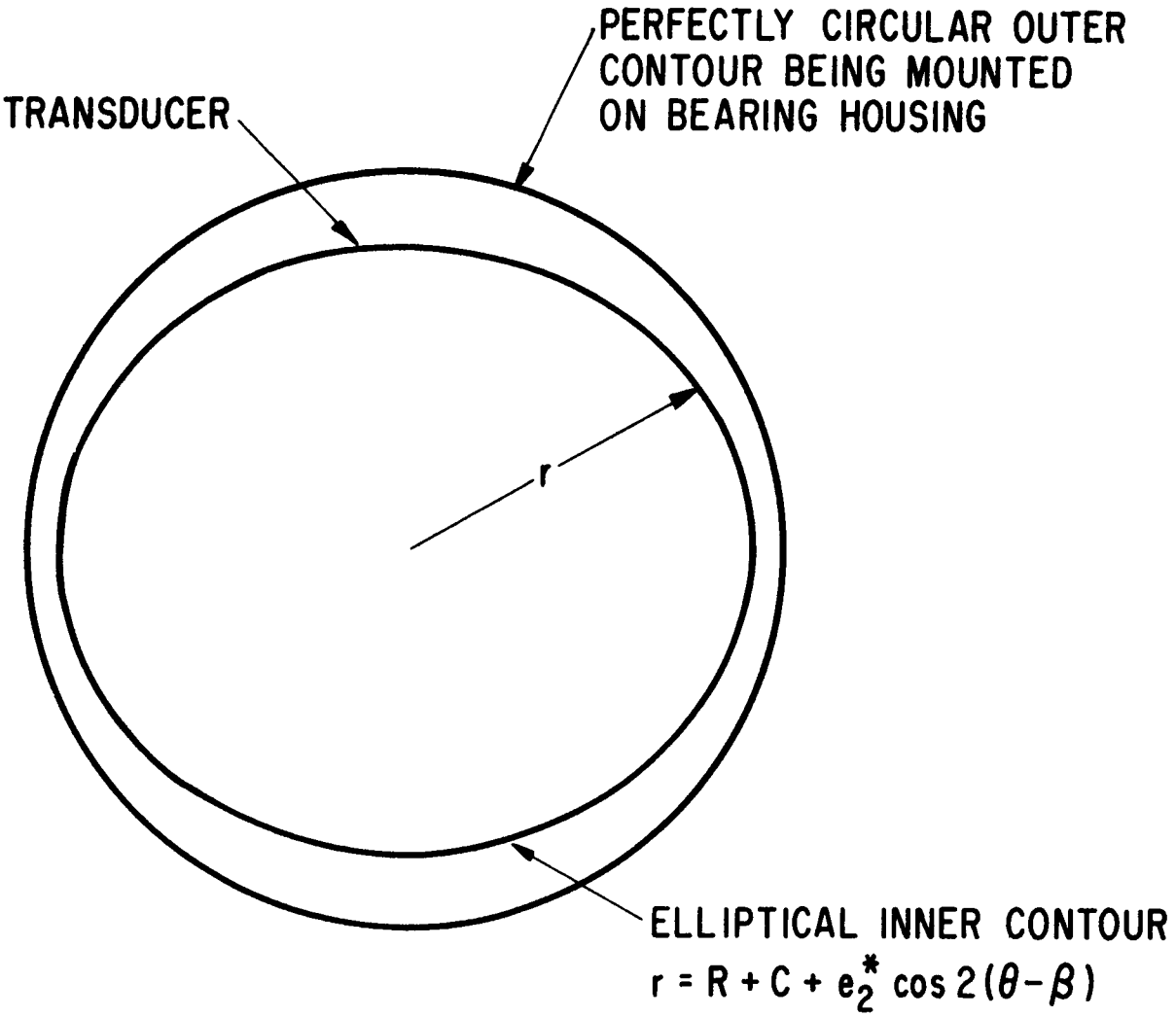

Fig. 8 Diagram illustrating non-uniform thickness of the transducer